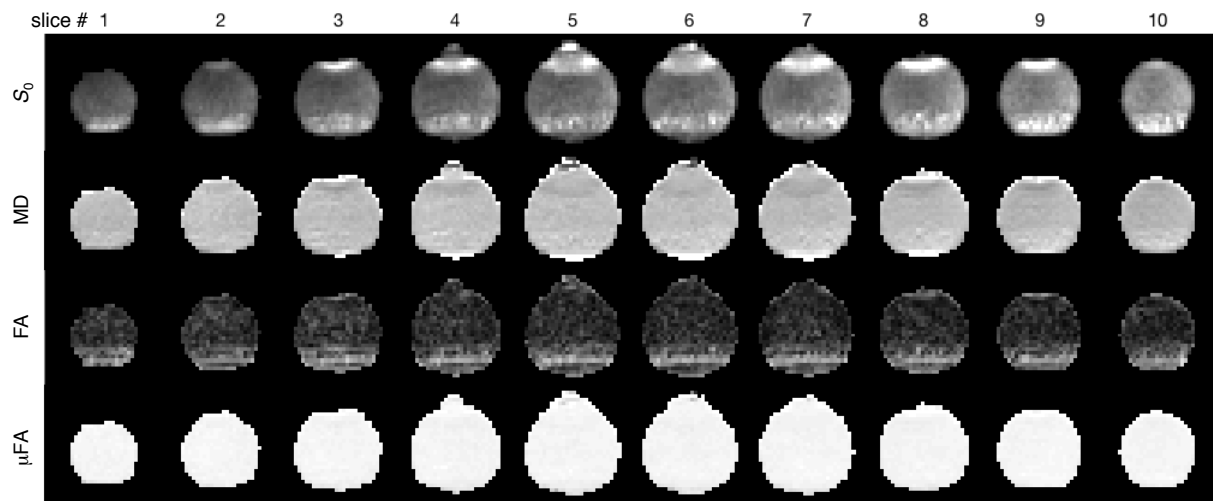
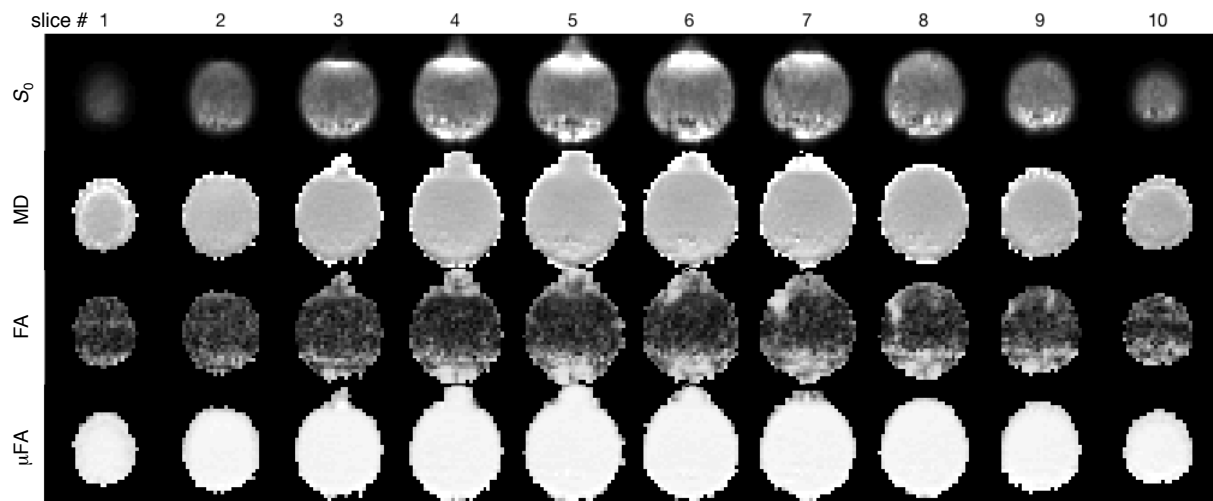


Supporting Table S1. Temperature stability range of the reverse hexagonal phase for samples with chemical compositions at and around the value chosen for the phantom.

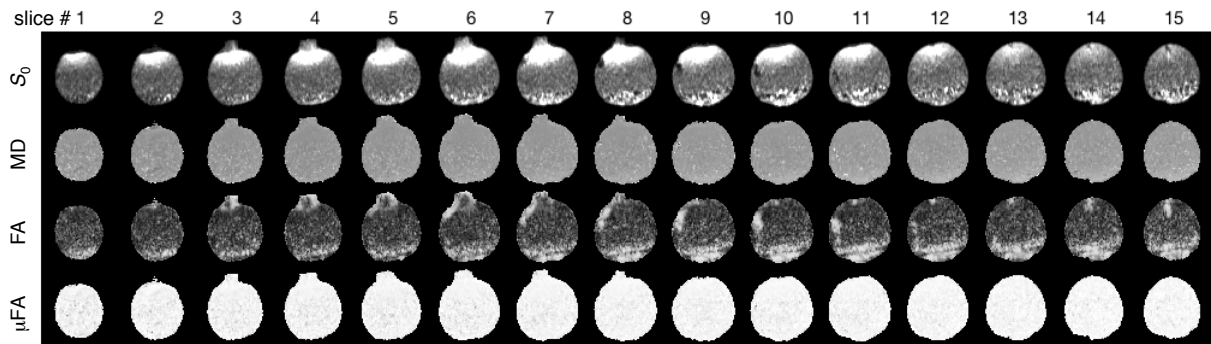
Chemical composition (wt%)			Temperature range (°C)	
AOT	isooctane	water	Lower limit	Upper limit
47.91	15.12	36.97	<5	29.0
46.00	14.52	39.47	<5	30.0
44.70	14.11	41.19	<5	30.0
44.12	13.94	41.94	<5	31.0
43.43	13.71	42.86	<5	31.5
41.79	13.19	45.02	<5	32.0



Supporting FIG. S1. Parameter maps for all slices of the experimental data in FIG. 4. The  $S_0$ , MD, and  $\mu$ FA maps were obtained with the *gamma* model, while the FA map is from standard *DTI* analysis. The gray scales have the same meanings as in FIG. 4.



Supporting FIG. S2. Demonstration of the long-time stability of the phantom. The data was acquired one year after the original measurements reported in FIG. 4 and Supporting FIG. S1 using the same scanner, experimental settings, and data processing pipeline. The gray scales have the same meanings as in FIG. 4. Note that the  $\mu$ FA maps remain uniform with values near unity.



Supporting FIG. S3. Application of the phantom on a conventional MR scanner. The data was acquired with the same phantom in Supporting FIG. S2 using a conventional Siemens Magnetom Prisma 3T scanner with  $0.080 \text{ Tm}^{-1}$  maximum gradient strength and  $200 \text{ Tm}^{-1}\text{s}^{-1}$  slew rate at a spatial resolution of  $2.0 \times 2.0 \times 4.0 \text{ mm}^3$  using an optimized acquisition protocol as described in Ref. (98). The data processing pipeline and visualization was the same as in Supporting FIG. S1. Note the uniformity of the  $\mu\text{FA}$  maps with values near unity.